
Observations from the Hinotori Mission [and Discussion]

Takashi Sakurai, A. G. Emslie, D. Alexander and E. R. Priest

Phil. Trans. R. Soc. Lond. A 1991 **336**, 339-347

doi: 10.1098/rsta.1991.0085

Email alerting service

Receive free email alerts when new articles cite this article - sign up in the box at the top right-hand corner of the article or click [here](#)

To subscribe to *Phil. Trans. R. Soc. Lond. A* go to:
<http://rsta.royalsocietypublishing.org/subscriptions>

Observations from the *Hinotori* mission

BY TAKASHI SAKURAI

National Astronomical Observatory, Mitaka, Tokyo, Japan

The satellite *Hinotori* was launched in 1981 by the Institute of Space and Astronautical Science of Japan. Two major experiments on board the *Hinotori* satellite were a hard X-ray imaging telescope with modulation collimators, and a high dispersion soft X-ray crystal spectrometer utilizing the Bragg diffraction of X-rays on quartz crystals. These two instruments have revealed for the first time that solar flares show varying characteristics depending on the environment of flaring regions, and that flares produce plasmas as hot as $3\text{--}4 \times 10^7$ K.

1. Introduction

The satellite *Astro-A* was the seventh satellite (and the first satellite dedicated to solar flare research) launched by the Institute of Space and Astronautical Science of Japan (Kondo 1982). After its launch on 21 February 1981, it has been given the name *Hinotori*, meaning 'fire-bird' in Japanese. The satellite carried 51 kg of scientific payload in the body of 106 cm diameter and 85 cm height; its total weight was 188 kg (figure 1). The orbit was roughly 600 km above the ground, and the orbital period was about 96 min. The attitude of the satellite was stabilized by its spin of about 4 r.p.m.

The scientific goal aimed at in the *Hinotori* project was to investigate high-energy phenomena in solar flares. The satellite had one imaging instrument, the hard X-ray telescope, with modulation collimators. The other instruments had no spatial resolution, and covered a range of wavelengths from soft X-rays to gamma rays. Among these, a soft X-ray crystal spectrometer utilizing the Bragg diffraction of X-rays performed high dispersion spectroscopy of spectral lines.

In June 1982 the data recorder on board *Hinotori* lost its function. For a few months the observations were continued during the satellite's passage over Japan, and finally the operation of *Hinotori* was shut down on 11 October 1982. During its mission of 20 months, *Hinotori* observed more than 700 flares. An extensive review of the results from the *Hinotori* mission was given by Tanaka (1987).

2. Hard X-ray imaging of solar flares

Usual optics (mirrors, etc.) cannot be used to make images in hard X-rays (energies above 10 keV). The hard X-ray telescope on board *Hinotori* utilized the modulation collimator (Oda collimator). The detector, a NaI scintillation proportional counter, by itself has no spatial resolution. When it sees the sun through two layers of fine grids, part of the sun is blocked by the grids, while the rest is visible from the detector. If one makes this transmission pattern move on the sun, one will obtain a one-dimensional scan of a solar X-ray image. Such an attempt was first made from a balloon-borne instrument (Takakura *et al.* 1971) and the location of a hard X-ray source in a flare was determined.

Phil. Trans. R. Soc. Lond. A (1991) **336**, 339–347

Printed in Great Britain

339

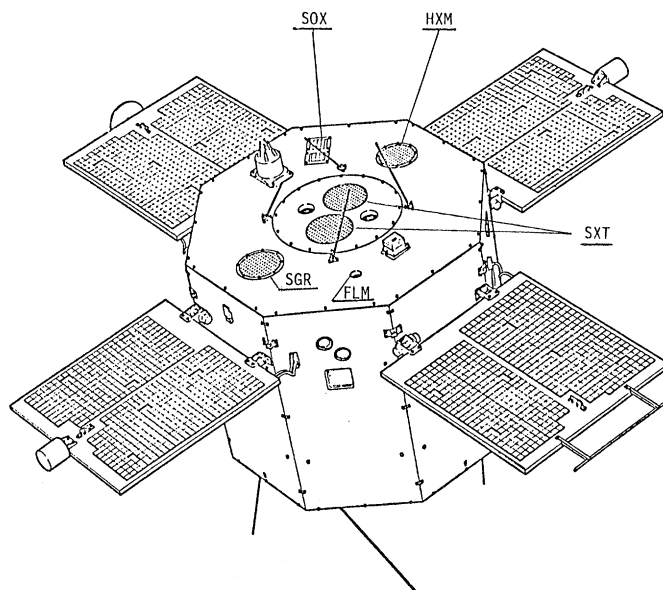


Figure 1. The *Hinotori* spacecraft. The hard X-ray telescope (SXT) is situated at the centre of the satellite. The other instruments are: Bragg crystal spectrometer (SOX), soft X-ray spectrometer (FLM), hard X-ray spectrometer (HXM), and gamma ray detector (SGR).

The instrument on *Hinotori* made use of the spin of the satellite for scanning. The axis of the telescope, which was co-aligned with the spin axis, was offset from the Sun centre by about 1.2° . A two-dimensional image scan was therefore made every 8 s (half of the spin period). The exact position of the telescope axis with respect to the sun was determined by using an optical aspect sensor co-aligned with the X-ray telescope. The instrument was made of two independent sets of grid-plus-detector assembly. The detectors have two energy channels, namely 15–40 keV (hard) channel and 6–13 keV (soft) channel. The soft channel was only occasionally used in the decay phase of flares.

Because good counting statistics were needed for image synthesis, only the images of relatively intense flares were obtained. Takakura *et al.* (1984) studied 30 flares for which X-ray imaging was possible. The achieved spatial resolution is 10 arcsec, which is modest compared with the resolution of optical observations from the ground. In most cases the hard X-ray sources only showed up as single sources. In such cases the size and the location of the sources with respect to optical images were obtained. The height of X-ray sources when flares took place near the solar limb yielded definite information on where in the solar atmosphere the X-rays are emitted.

From the observations it is inferred that in most flares the hard X-ray sources are in the corona, 10^4 km or more above the solar surface. If the flare takes place in a magnetic loop, the brightest location in X-rays is not at the loop footpoints near the chromosphere, but near the top of the loop or the loop as a whole brightens. This means that the high energy electrons of around 20 keV, which are responsible for the X-rays detected by the *Hinotori* telescope, do not reach the loop footpoints if beams of accelerated electrons are produced near the loop top. This is consistent with the estimated density and length of the flaring loop. For less dense or shorter loops the emission from the footpoints will be more enhanced. Such examples, with footpoint emission, were also found, though less frequently. (If the detector had been more

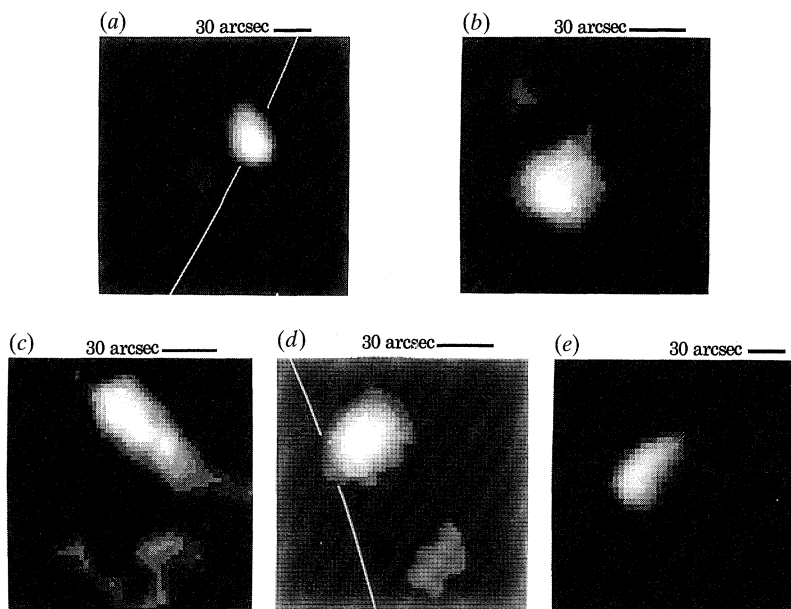


Figure 2. A collection of hard X-ray images taken by the X-ray telescope on board *Hinotori* (Sakurai 1985). The scale is indicated on each image. The flares in the top row are impulsive flares, while those in the bottom row are gradual hard flares. The solar limb is indicated for the flares close to the limb. (a) 20 July 1981, UT 13:15:48; (b) 15 October 1981, UT 04:44:10; (c) 1 April 1981, UT 01:30:09; (d) 27 April 1981, 07:56:18; (e) 13 May 1981, UT 04:13:12.

sensitive to higher energy X-rays, the telescope would have seen the X-ray emission more concentrated near the loop footpoints.) On the other hand there is a class of flares with very soft X-ray spectrum which presumably originates from a 'super-hot' (greater than 3×10^7 K) plasmas. These 'hot thermal flares' (Tanaka *et al.* 1982; Tsuneta *et al.* 1984b) are characterized by a compact source in the corona which might indicate small and dense loops.

In a limited number of cases the X-ray sources were made of several separate sources, or the sources were large enough that one could see the structure of the sources (figure 2). These X-ray flares tend to delineate the $H\alpha$ flare ribbons, indicating that the X-ray sources are in magnetic arcades over the magnetic neutral line. There is a particular class of X-ray flares which are located high in the corona (greater than 3×10^4 km) and emit hard X-rays of non-thermal (power-law) spectrum. Strong microwave emission (due to the gyro-synchrotron mechanism of accelerated electrons in a magnetic field) is observed from this class of flares. These 'gradual hard flares' (Tsuneta *et al.* 1984a) are characterized by low density loops with the trapping of high energy particles by magnetic mirroring.

One of the most interesting findings of *Hinotori* is that hard X-ray sources show a variety of forms as described above. As will be discussed in §4, this diversity of hard X-ray flares can be interpreted in terms of the environmental condition of the flaring region.

3. X-ray spectroscopy of solar flares

(a) Line spectroscopy

The spectroscopy of emission lines from hot plasmas yields information on the temperature, density, ionization stage, elemental abundance and the Doppler shift of the plasmas. The measurement is made by using the X-ray diffraction on a crystal (i.e. the Bragg diffraction). The wavelength of X-rays which are reflected by the crystal is a function of the angle of incidence of the X-rays with respect to the crystal. To scan the wavelength one must either rotate the crystal mechanically, or bend the crystal so that every small part of the crystal has a different incidence angle of X-rays. In the *Hinotori* instrument, the spectrometer was fixed to the satellite body, and the satellite spun around its axis which was pointed 1.2° off the Sun's centre.

This novel scheme of wavelength scanning was tested on similar spectrometers flown on MS-T4 (*Tansei-IV*) satellite, one year before the launch of *Hinotori*. (*Tansei* means 'light blue' in Japanese, the symbolic colour of Tokyo University). Two sets of LiF crystal were used to observe the wavelength regions $1.8\text{--}2.0\text{ \AA}$ † and $3.1\text{--}3.25\text{ \AA}$, which contain lines of highly ionized iron ($\text{Fe}^{\text{XXI}}\text{--}\text{Fe}^{\text{XXV}}$) and calcium (Ca^{XIX}) respectively. The wavelength resolutions were 0.5 m\AA and 0.4 m\AA in the two respective bands.

The Bragg crystal spectrometer on *Hinotori* consisted of two systems: the higher resolution detector covered $1.83\text{--}1.89\text{ \AA}$ with the resolution of 0.15 m\AA , and the lower resolution detector covered $1.75\text{--}1.95\text{ \AA}$ with 2 m\AA resolution. Both systems used quartz crystals and NaI scintillation counters. The observed wavelength regions contain emission lines of iron whose ionization stages are up to Fe^{XXV} (helium-like ion) and Fe^{XXVI} (hydrogen-like ion).

It has been known since the 1970s that flares produce plasmas of $1\text{--}2 \times 10^7\text{ K}$. Most flares show this range of temperature from the beginning, or in other words the sensitivity of the spectrometers is not enough in detecting the initial rise in temperature. The Bragg crystal spectrometers on *Tansei-IV* had high enough sensitivity, though the resolution was modest, and detected the initial temperature rise. In a timescale of 10 s, the dominant ionization stage of iron changed from Fe^{XXII} to Fe^{XXIV} , indicating the heating from below $1 \times 10^7\text{ K}$ to $2 \times 10^7\text{ K}$ (Tanaka 1980). Under such a rapid heating, there exists the possibility that the plasma may deviate from thermal equilibrium. In the *Hinotori* spectra, which had higher spectral resolution, an indication of non-equilibrium (transient) ionization was found (Doschek & Tanaka 1987).

The temperature of flare plasma can be obtained by measuring the intensity ratios of relevant spectral lines. The temperature values thus obtained from the ions up to Fe^{XXV} are mutually consistent and in the range of $1\text{--}2 \times 10^7\text{ K}$. However, the temperature derived from Fe^{XXVI} spectra sometimes showed a higher temperature ($3\text{--}4 \times 10^7\text{ K}$) in the most intense phase of flares. In such a phase the flare plasma might consist of two components, one in $1\text{--}2 \times 10^7\text{ K}$ and the other in $3\text{--}4 \times 10^7\text{ K}$. The latter component was discovered for the first time in the 1980s, and is referred to as the super-hot component. Earlier evidence for this component is given by Lin *et al.* (1981) and Hoyng *et al.* (1981).

The ratio of ionization population $[\text{Fe}^{\text{XXVI}}]/[\text{Fe}^{\text{XXV}}]$ determined from the spectra of the *Hinotori* instrument is several times greater than the value expected in thermal

† $1\text{ \AA} = 10^{-10}\text{ m} = 10^{-1}\text{ nm}$.

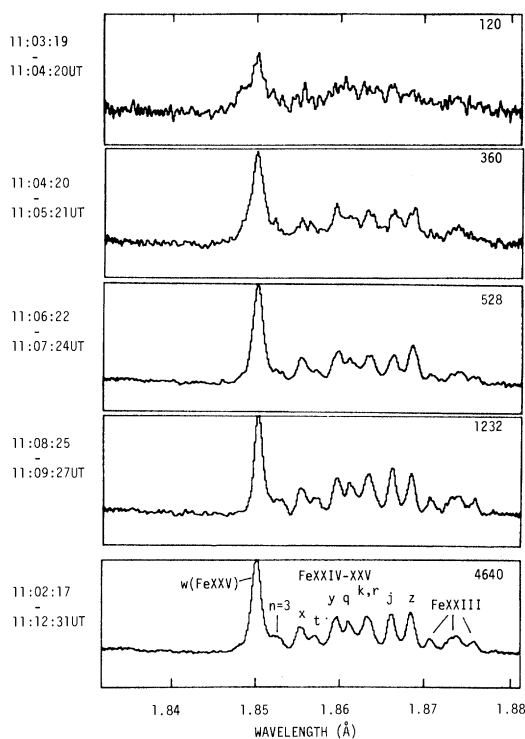


Figure 3. The spectra of highly ionized iron in the wavelengths 1.8–2 Å, as a function of time (Tanaka *et al.* 1982). The blue-shift and the broadening of the Fe^{XXV} line is seen in the initial phase of this flare.

equilibrium (of the temperature derived from Fe^{XXV}). This tendency is not restricted to the most intense phase of flares but can be seen in the entire flare phases. The introduction of several components with differing temperatures will not resolve this discrepancy. The uncertainty in the atomic physics constants will only introduce a discrepancy of factor two at most. Kato & Masai (1991) proposed that this behaviour can be explained if the flare plasma is not in thermal equilibrium. By assuming the existence of a super-thermal population of electrons (with a temperature of about 10 keV occupying a volume of a few percent), they were able to reproduce the behaviour of the observed ionization population ratio.

The spectral lines also give information on the motion of plasmas. In the initial phase of flares the Fe^{XXV} lines are found to be blue-shifted, that is, the X-ray emitting plasmas move upward from the solar surface (figure 3). This phenomenon has been expected from indirect observations and theoretical considerations and is called 'the chromospheric evaporation'. In this (rather loose) terminology, the dense chromosphere is regarded as liquid in contrast to the hot flare plasma in the corona: the heat from the hot gas evaporates the cool chromosphere. The upward velocity reaches 400 km s^{-1} in the initial phase of flares, and decreases toward the later phase to less than 200 km s^{-1} . The width of these spectral lines is also very broad in the initial phase, and the equivalent ion temperature is as large as 10^8 K . It is therefore more likely that this width represents unresolved random motion of gases. The velocity of the random motion is of the order of 100 km s^{-1} , and decreases in the later phase. In flares taking place near the solar limb, broadened spectral lines persist

(Tanaka 1986) but the blue-shift diminishes (Antonucci & Dennis 1983). Therefore the blue-shift represents a systemic upflow (or flow along nearly vertical magnetic tubes), while the broadening of the lines is due to more or less isotropic and random motion of gases.

(b) Continuum spectroscopy

The wide-band spectrometers on *Hinotori* covered three energy ranges. The detector for the lowest, soft X-ray energy band (2–12 or 2–20 keV) is made of a gas scintillation proportional counter filled with xenon gas. The energy resolution is $\Delta E/E = 10\%$ at 6 keV, which is twice as good as the ordinary proportional counter. The same type of detectors were also used in the *Astro-B (Tenma)* mission for cosmic X-ray study, and yielded significant progress in the study of high temperature plasmas in close binary systems (Nagase 1989). From the soft X-ray continuum spectra obtained by *Hinotori*, one can derive the temperature and the emission measure of X-ray emitting plasmas. The computed spectra by assuming a temperature of $1\text{--}2 \times 10^7$ K generally give satisfactory fit to the observed data (Watanabe *et al.* 1983). Some discrepancy is found in the energies above 10 keV, which could either be due to the super-hot component or due to non-thermal X-rays.

The hard X-ray energy range (17–340 keV in seven channels) was observed by a NaI scintillation counter. By combining the soft and hard X-ray spectrometer data, one can trace the time evolution of thermal plasmas and non-thermal electrons (with a power law energy spectrum). Generally the changeover from thermal to non-thermal spectra takes place at about 20 keV. However, in some flares the power-law component could be traced down to the 10 keV range (Watanabe *et al.* 1983; Tanaka *et al.* 1984a). If literally interpreted, in such flares the total energy of non-thermal electrons may exceed that of thermal electrons by a large factor. This may invalidate the otherwise most probable picture that the energy of electron beams is ultimately converted into the thermal energy of plasma.

The gamma rays in the energy range 0.2–6.7 MeV were measured by a CsI scintillation counter. The simultaneity of proton acceleration and electron acceleration, which are responsible for gamma and X-ray emissions respectively, was first discovered by the *SMM* satellite and was confirmed by *Hinotori* (Yoshimori *et al.* 1983). For long duration events (gradual hard flares), the delay of peaks in gamma rays with respect to X-rays was observed, which is in accord with the classical two-step acceleration of high energy particles in solar flares.

4. A synthetic view of solar flares

From the results obtained with the *Hinotori* instruments, we can derive a synthetic view of the solar flare. The primary energy release may or may not be due to a single mechanism. But at least a variety of flare characteristics might be explained in terms of differing environments at the flare site. The majority of flares, which are called impulsive flares, produce accelerated electrons which stream down to the chromosphere. The heated chromospheric material rises with the velocity of a few hundred kilometres per second. This upflow is the major supplier of mass in the flare. Subsequently, the flaring loop is filled with the evaporated plasma of $1\text{--}2 \times 10^7$ K. The continued energy release may heat this plasma to a higher temperature ($3\text{--}4 \times 10^7$ K), especially at the energy liberation site presumably near the top of the

loop. From observations of the flares which occurred behind the limb, the evaporation component lies closer to the solar surface while the super-hot component is situated high in the corona.

If the loop is dense at the beginning of a flare, electrons may either be heated instead of being accelerated, or may be accelerated first but may thermalize before reaching the chromosphere. Such a flare is called the hot thermal flare. The hard X-ray images of this class of flares are compact, indicating a localized region of very high density. Chromospheric material will be heated by a heat conduction front created at the energy liberation site, and the evaporation will add further mass to the flaring loop.

Hard X-rays of non-thermal origin are produced in the gradual hard flares. These flares are explained by continued energy release (particle acceleration) in a low density, tall loop (or arcade of loops). A factor which distinguishes the gradual hard flare from most common impulsive flares might be the magnetic field configuration (Sakurai 1985). A magnetic loop with larger mirror ratio (i.e. a strongly constricted loop) is more favourable for the trapping of high-energy particles. The trapping will explain strong microwave radio emission from this class of flares (Kawabata *et al.* 1983). The constriction of magnetic fields will tend to inhibit high-energy electrons from reaching the chromosphere. The loop may be kept in relatively low density because of this effect. The energy partitioning into thermal, non-thermal and bulk energies might also be controlled directly by the primary energy liberation mechanisms. This point is not disentangled from environmental factors in the observations made by *Hinotori*. This is partly because the *Hinotori* mission lacked the capability of obtaining the images of the pre-flare corona. The location of the flare site in terms of the pre-flare structure was not known, neither the thermal nor the dynamical evolution of magnetic loops leading to a flare was observed. These shortcomings will be greatly improved in the missions in the present solar maximum.

The most significant outcome of the *Hinotori* experiment is that complex behaviour of solar flares has been sorted out and attributed to a few basic processes. In this respect the *Hinotori* mission has advanced the frontier of solar flare research to an unprecedented degree.

The *Hinotori* mission is the result of the effort of many people, and the author is thankful to those who contributed to this successful project. A review like this should have been written by the late Professor Katsuo Tanaka, who died on 2 January 1990 at the age of 46. He himself designed the Bragg crystal spectrometers on *Tansei-IV* and *Hinotori*, and had played a leading role in the *Hinotori* science team. This article is dedicated to his memory.

References

- Antonucci, E. & Dennis, B. R. 1983 Observation of chromospheric evaporation during the Solar Maximum Mission. *Solar Phys.* **86**, 67–77.
- Doschek, G. A. & Tanaka, K. 1987 Transient ionization and solar flare X-ray spectra. *Astrophys. J.* **323**, 799–809.
- Hoyng, P., Duijveman, A., Machado, M. E., Rust, D. M., Svestka, Z., Boelee, A., de Jager, C., Frost, K. J., Laffleur, H., Simnett, G. M., van Beek, H. F. & Woodgate, B. E. 1981 Origin and location of the hard X-ray emission in a two-ribbon flare. *Astrophys. J.* **246**, L155–L159.
- Kato, T. & Masai, K. 1991 X-ray spectra from *Hinotori* satellite and suprathermal electrons. In *Proc. Int. Solar-A Science Meeting on Flare Physics in Solar Activity maximum 22* (ed. Y. Uchida, R. C. Canfield, E. Hiei & T. Watanabe). Tokyo: Springer-Verlag. (In the press.)

- Kawabata, K., Ogawa, H. & Suzuki, I. 1983 A flare model deduced from Hinotori and millimeter wave interferometer observations. *Solar Phys.* **86**, 247–252.
- Kondo, I. 1982 On the system and operation of Hinotori. In *Hinotori Symp. on Solar Flares* (ed. Y. Tanaka), pp. 3–13. Tokyo: Institute of Space and Astronautical Science.
- Lin, R. P., Schwartz, R. A., Pelling, R. M. & Hurley, K. C. 1981 A new component of hard X-rays in solar flares. *Astrophys. J.* **251**, L109–114.
- Nagase, F. 1989 Accretion-powered X-ray pulsars. *Publ. Astron. Soc. Japan* **41**, 1–80.
- Sakurai, T. 1985 Magnetic field structures of hard X-ray flares observed by Hinotori spacecraft. *Solar Phys.* **95**, 311–321.
- Takakura, T., Ohki, K., Shibuya, N., Fujii, M., Matsuoka, M., Miyamoto, S., Nishimura, J., Oda, M., Ogawara, Y. & Ota, S. 1971 The location and size of a solar hard X-ray burst on September 27, 1969. *Solar Phys.* **16**, 454–464.
- Takakura, T., Tanaka, K. & Hiei, E. 1984 High temperature phenomena in flares. *Adv. Space Res.* **4**, 143–152.
- Tanaka, K. 1980 Soft X-ray line emission from solar flares. In *Proc. Japan–France Seminar on Solar Physics* (ed. F. Moriyama & J. C. Henoux), pp. 219–228. Tokyo: Tokyo Astronomical Observatory.
- Tanaka, K. 1986 Solar flare X-ray spectra of Fe XXVI and Fe XXV from the Hinotori satellite. *Publ. Astron. Soc. Japan* **38**, 225–249.
- Tanaka, K. 1987 Impact of X-ray observations from the Hinotori satellite on solar flare research. *Publ. Astron. Soc. Japan* **39**, 1–45.
- Tanaka, K., Watanabe, T., Nishi, K. & Akita, K. 1982 High-resolution solar flare X-ray spectra obtained with rotating spectrometers on the Hinotori satellite. *Astrophys. J.* **254**, L59–L63.
- Tanaka, K., Watanabe, T. & Nitta, N. 1984 Solar flare iron K α emission associated with a hard X-ray burst. *Astrophys. J.* **282**, 793–798.
- Tsuneta, S., Nitta, N., Ohki, K., Takakura, T., Tanaka, K., Makishima, K., Murakami, T., Oda, M. & Ogawara, Y. 1984a Hard X-ray imaging observations of solar hot thermal flares with the Hinotori spacecraft. *Astrophys. J.* **284**, 827–832.
- Tsuneta, S., Takakura, T., Nitta, N., Ohki, K., Tanaka, K., Makishima, K., Murakami, T., Oda, M., Ogawara, Y. & Kondo, I. 1984b Hard X-ray imaging of the solar flare on 1981 May 13 with the Hinotori spacecraft. *Astrophys. J.* **280**, 887–891.
- Watanabe, T., Tanaka, K., Akita, K. & Nitta, N. 1983 Thermal evolution of flare plasma. *Solar Phys.* **96**, 107–113.
- Yoshimori, M., Okudaira, K., Hirasima, Y. & Kondo, I. 1983 Gamma-ray observations from Hinotori. *Solar Phys.* **86**, 375–382.

Discussion

A. G. EMSLIE (*University of Alabama, Huntsville, U.S.A.*) To what extent does cooling of super-hot material, as opposed to heating of chromospheric material, contribute to the growth of the 20 million degree soft X-ray component?

T. SAKURAI. The emission measure of the super-hot component is generally an order of magnitude smaller than that of the normal hot component ($1\text{--}2 \times 10^7$ K). Therefore the normal component is not explained in terms of the super-hot component that had cooled off. The mass of the normal component is believed to be primarily supplied by the chromospheric evaporation. The major energy loss of the super-hot component is due to thermal conduction and not due to radiative cooling.

D. ALEXANDER (*University of Glasgow, U.K.*). The non-thermal energy you measure in the iron lines, equivalent to velocities of 100 km s^{-1} , is at least comparable with the thermal energy in these lines. A similar result was found by J. Saba and K. T.

Strong in their studies of active regions. Could you comment, and did your results display any correlation between flare intensity and the derived non-thermal velocity?

T. SAKURAI. Non-thermal line broadening observed by *Hinotori* showed poor correlation with flare intensity. (Flares of similar intensity showed various magnitude of line broadening.) A tendency was reported that the flares which are confined within a small volume show larger line broadening (Tanaka 1986).

E. R. PRIEST (*The University, St Andrews, U.K.*). (i) What are the typical heights of your three kinds flare? Which of them are two-ribbon events? (ii) Do you see any of your X-ray sources rise in altitude during the flare, as in the classical soft X-ray behaviour during two-ribbon events? (iii) Do you even observe red shifts?

T. SAKURAI. (i) All the gradual hard flares observed by *Hinotori* were two-ribbon flares. Most of the other two types (impulsive flares and hot thermal flares) observed by *Hinotori* were also two-ribbon flares. The X-ray classification of flares introduced by *Hinotori* observations may not be directly related to whether a flare is compact or two-ribbon (whether the magnetic field is closed or open). (The heights of flare sources were discussed in the text.) (ii) The rising motion of X-ray sources was observed in many flares. We also observed flares which showed stable X-ray sources in the corona. (iii) As far as I know, no red shifts in flares were observed by the Bragg crystal spectrometer of *Hinotori*.

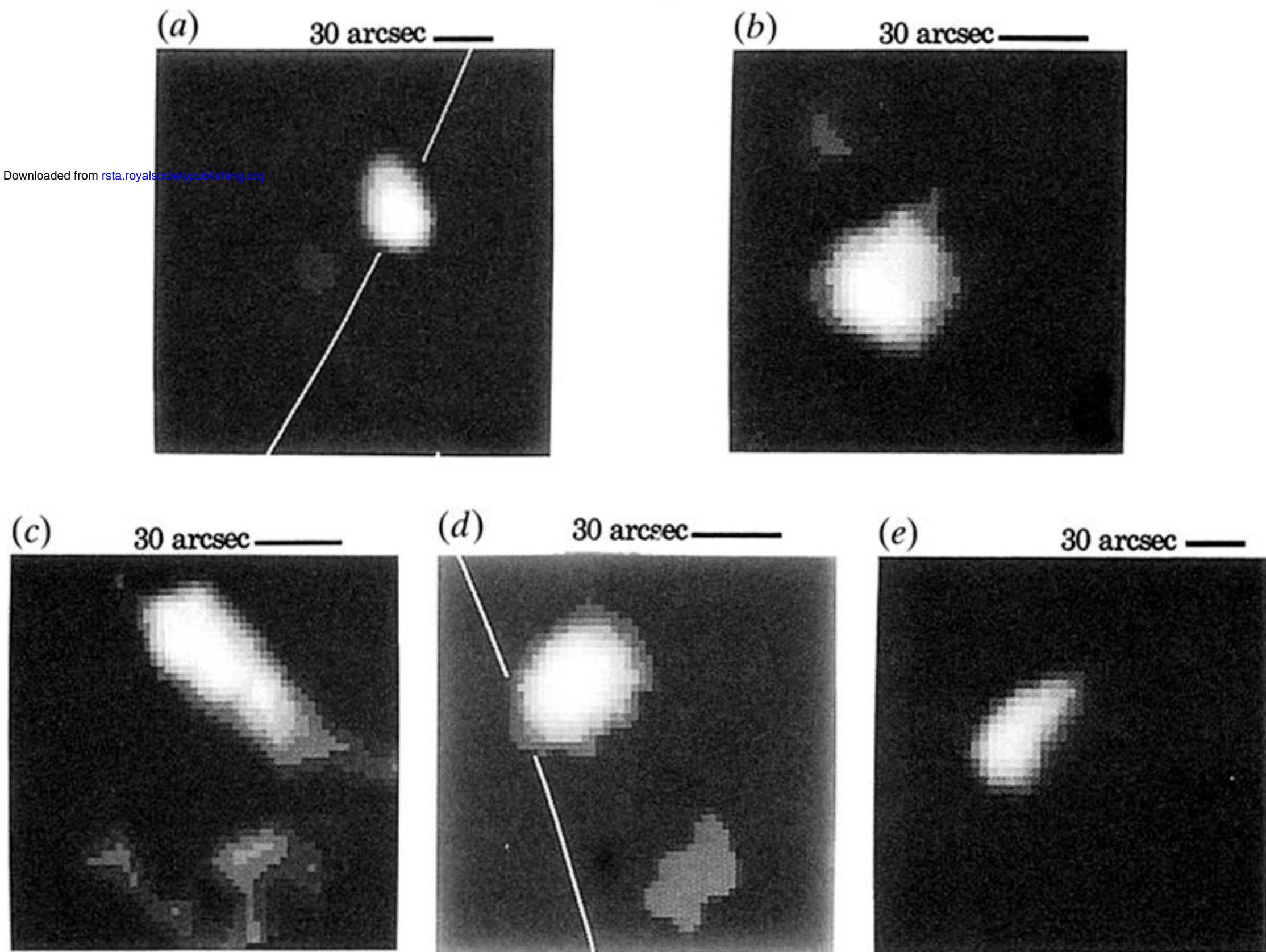


Figure 2. A collection of hard X-ray images taken by the X-ray telescope on board *Hinotori* (Sakurai 1985). The scale is indicated on each image. The flares in the top row are impulsive flares, while those in the bottom row are gradual hard flares. The solar limb is indicated for the flares close to the limb. (a) 20 July 1981, UT 13:15:48; (b) 15 October 1981, UT 04:44:10; (c) 1 April 1981, UT 01:30:09; (d) 27 April 1981, 07:56:18; (e) 13 May 1981, UT 04:13:12.